APPLICATION OF STATIC STATE ESTIMATOR ON INDUCTION FURNACE

By

Ahmed A. Al – Rajihy
College of Engineering,
University of Kerbala

Ala M. Hussein Al – Jessany,
Hazim Wally Chillab
College of Engineering,
University of Babylon

ABSTRACT

A mathematical model for calculating the temperature distribution during induction heating of a cylindrical charge has been made. In this model the temperatures of the charge at five nodes are the fundamental variables. A finite element analysis has been made for the melting process of the furnace charge for two materials which are aluminum and iron. This model was used as a reference for the performance of the estimator.

A static state estimator with a measurement redundancy of 3.33 for the induction furnace has been developed. Numerical tests show that the static state estimator is satisfactory for the use in state estimation, the weighted least squares WLS approach is an effective technique in estimation, and the criterion proposed in this work is effective for the identification process when bad data exist.

Keywords

الخلاصة

تم عمل نموذج رياضي لحساب توزيع درجات الحرارة لشحنة فرن حث كهربائي حيث ان درجات الحرارة لمادة الشحنة لخمس مواقع في الشحنة هي المتغيرات الأساسية. تم دراسة وتحليل عملية صهر شحنة الفرن لمادتين هما الألمنيوم والحديد كلا" على حدة، وتم اعتماد هذا النموذج كأساس لتقييم كفاءة و أداء المخمن.

تم تطوير مخمن ستاتيكي بفائض قياسات مقداره 3.33 لفرن الحث. وقد أظهرت النتائج كفاءة هذا المخمن في عملية تخمين درجة حرارة الشحنة، و أن طريقة مربعات الفروقات الموزونة WLS هي طريقة ذات كفاءة عالية في عملية التخمين. لقد تمكن المخمن من رصد وتحديد مواقع القراءات الخاطئة (في حالة وجودها) بشكل جيد وحذفها ومن ثم تعوض هذه القراءات المخطوءة بأخرى صحيحة.

I- INTRODUCTION

State estimation is the process of assigning a value to an unknown system state variable based on measurements from that system according to some criteria. Usually, the process involves imperfect measurements that are redundant and the process of estimating the system state is based on a statistical criterion that estimates the true value of the state variables to minimize or maximize the selected criterion. A commonly used and familiar criterion is the weighted least squares approach (WLS) which is based on minimizing the sum of the squares of the differences between the estimated and " actual" (i.e. measured) values of functions. A very useful feature of a state estimation calculation is the ability to calculate (or estimate) quantities not being measured. This is most useful in cases of failure of communication lines connecting transducers to thermal processor or when the transducer fails. A state estimator can “smooth out” small random errors in sensor readings, detect and identify gross measurement errors and “fill in” instrument readings that have failed due to communication failures, or any other malfunction.

State estimators may be either of a static or dynamic type. This research is concerned with the development of a static state estimator, capable of predicting (estimating) charge temperature of an induction furnace. The estimator is developed to produce the “best estimate" of the furnace temperatures and power supply recognizing that there are errors in the measured quantities and that there may be redundant measurements. The output data can then be used in other thermal processor functions such as the control of the melting process.

Baker [1] referred to the analytical solution of classical heat flow problem as a method of analyzing the more practical heat flow problems of induction heating. The solution of a long cylinder is given, initially at zero temperature, supplied with constant power at the surface, starting at time equal to zero. Theoretical results are favorably compared with the experimental results, and presented in a dimensionless form.

Lenden et al. [2] presented a comparison between three different methods for determining the thermal diffusivity of a long copper rod as an example of one dimensional heat diffusion process. The methods used are modified Angstrom's method, least square method, and maximum likelihood method, which have been applied to data obtained from experiments on a long copper bar. The comparison based on the accuracy, the amount of computation, the storage capacity, and in general the advantages and the limitations of each method. The results showed that the maximum likelihood method provides greater accuracy but more computational time and storage than the other methods.

Potapov et al. [3] presented a theoretical modeling of the process of heating of a solid round billet in an induction furnace in order to develop optimum heating ensuring a minimum temperature difference over the cross-section of the billet. The heat flow assumed to be only in radial direction. Results of the calculations were in good agreement with the experimental data.

Al-Ubaidy [4] had used the state estimation technique in order to predict the temperature of an induction furnace charge. A finite element software package was used, the results are plotted in a dimensionless form. The numerical results are favorably compared with the analytical results obtained by Baker [1]. In the technique which was used the model was depending on a five elements state vector with a measurement redundancy equal to **two**. The results showed a good accuracy

The main goal of this work is to increase the redundancy measurements and to increase the accuracy of the estimator based on the techniques mentioned above.

II- SIMULATION OF THE FURNACE

For practical monitoring applications, the thermal system can be represented as a lumped system described by ordinary differential equations. The lumped thermal model assumes that the heat storage in a material can be represented by an effective thermal capacitance, C, and that the resistance to the heat flow between any two points can be represented by an effective thermal resistance, R. An analogy may be made to an electrical circuit, in which current represents heat flow and voltage represents temperature.

The lumped model approach results in first-order dynamics in the temperature response to the heat input for a given point, or node. For a single node, the heat balance is simply given by the normalized equation [5];

$$q_i = \frac{T(t) - T_a(t)}{R} + C\frac{dT(t)}{dt} \tag{1}$$

Where q_i is the power generated at node i. This equation may be written in a state variable form, anticipating the construction of a set of dynamic equations for describing temperature distribution in the charge of an induction furnace as;

$$\dot{T} = \frac{(T_a - T)}{RC} + \frac{q_i}{C} \quad (2)$$

Figure (1) shows one way in which the basic thermal network may be set on for a charge in a furnace. The charge is assumed to be insulated all around and heat will escape through the insulator (in radial direction) towards the cooling water by virtue of temperature difference.

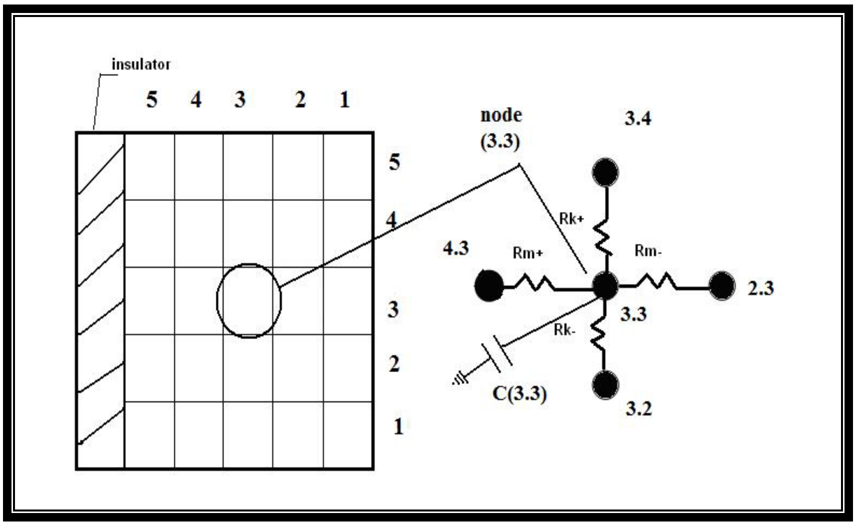

Figure (1): Equivalent R-C simulation of the charge

Following the approach represented by Eq. (2), the temperature dynamic equation for any node (node m,k) of the furnace charge can be written as:

$$\dot{T}_{m,k} = \frac{1}{C_{m,k}R_{m+1,k}}(T_{m+1,k} - T_{m,k}) + \frac{1}{C_{m,k}R_{m-1,k}}(T_{m-1,k} - T_{m,k}) + \frac{1}{C_{m,k}R_{m,k+1}}(T_{m,k+1} - T_{m,k}) + \frac{1}{C_{m,k}R_{m,k-1}}(T_{m,k-1} - T_{m,k}) + \frac{q_m}{C_{m,k}} \quad (3)$$

where,

$$C_{m,k} = \rho_{m,k} C_{p_{m,k}} \Delta V_{m,k} \text{,}$$

$$\Delta V_{m,k} = r_m \Delta r \Delta \phi \Delta z \text{,}$$

$$R_{m+1,k} = \frac{\Delta r}{(r_m + \Delta r/2)\Delta\phi\Delta z k_c} \text{,}$$

$$R_{m-1,k} = \frac{\Delta r}{(r_m - \Delta r/2)\Delta\phi\Delta z k_c} \text{,}$$

$$R_{m,k+1} = \frac{\Delta z}{r_m \Delta\phi \Delta r k_c} \text{,}$$

$$R_{m,k-1} = \frac{\Delta z}{r_m \Delta\phi \Delta r k_c},$$

And $q_m = q_i$

III- MEASUREMENT SYSTEM:

The measurement system model is very important for the function of the estimator itself and for the case of instrument or communication lines failure. The derivation of the measurement equations depends on the type of variable and the locations of the sensors. The principal quantities measured are temperatures, electric power and cooling water mass flow rate. Owing to the construction and operational conditions of the furnace, some quantities cannot be measured easily (mainly charge temperature). Each measurement can be expressed in the form of an equation. The equation will give the value of the measurement in terms of the state variables.

Figure (2) shows a sketch for the proposed locations of the set of the measuring sensors adopted for the design of a static state estimator for an induction furnace. It is assumed that the following quantities are measurable : the temperature of the insulator at nodes s_1, s_2, s_3, and s_4 (T_1, T_2, T_3 and T_4), the heat transferred from the charge towards the cooling water (Q_l), the temperatures of the water at the inlet and outlet of the cooling coil (T_{in} and T_{out}), the mass flow rate of the cooling water (M_w) and finally the electrical power (p_t) and the equivalent heat input at the terminals of the induction coil (P_{acl}).

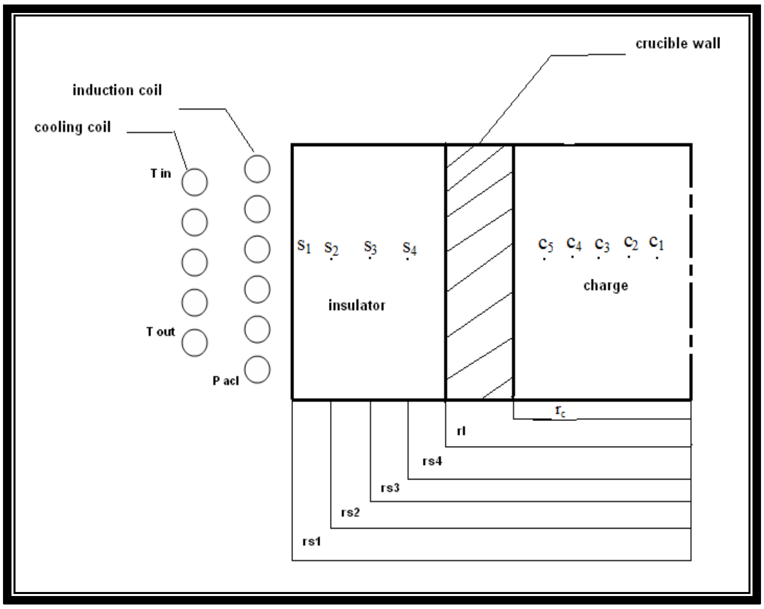

Figure (2): The proposed measuring system

In order to facilitate a mathematical formulation while still retaining the essential feature of the furnace, some assumptions have to be made:
1- The thermal properties of the charge, cooling water and the insulator are constant.
2- The kinetic and potential energies are neglected in the energy equations.

3- The mass flow rate of the cooling water is constant during the melting process.
To derive the measurement equations, the induction furnace is divided into three sections: crucible wall and the insulator, cooling coil, and induction coil as detailed in the following sections.

a- Crucible wall and the Insulator:

As shown in figure (2), four different positions inside the insulator are proposed to locate thermocouple junctions. These thermocouples provide an on-line temperature measurement to the estimator for the continuous prediction of the charge temperature.

In the steady state, the radial heat transfer equation can be applied in order to obtain the measurement equations which relates the temperatures at nodes s_1, s_2, s_3, and s_4 of figure (2) and the temperature at the surface of the charge T_c, which is given by:

$$T_c = (\text{heat generated} / M_c C_p) + T_{initial} \tag{4}$$

Since the heat lost through the crucible wall and the insulator is constant, so the temperature at the node s_1 of the insulator is given by:

$$\frac{2\pi l_w (T_c - T_1)}{\frac{1}{k_z}\ln\frac{r_l}{r_c} + \frac{1}{k_{ins}}\ln\frac{r_{s1}}{r_l}} = \frac{2\pi l_w (T_c - T_{in})}{\frac{1}{k_z}\ln\frac{r_l}{r_c} + \frac{1}{k_{ins}}\ln\frac{r_{ins}}{r_l} + \frac{1}{k_{cu}}\ln\frac{r_w}{r_{ins}}} \tag{5}$$

let,

$$haz = \frac{1}{k_z}\ln\frac{r_l}{r_c} + \frac{1}{k_{ins}}\ln\frac{r_{ins}}{r_l} + \frac{1}{k_{cu}}\ln\frac{r_w}{r_{ins}}$$, and

$$b = \frac{1}{k_z}\ln\frac{r_l}{r_c} + \frac{1}{k_{ins}}\ln\frac{r_{s1}}{r_l}$$

Solving Eq. (5) for T_1 and simplifying with the above substitutions, the following equation can be obtained:

$$T_1 = T_c - \frac{T_c - T_{in}}{haz} b \tag{6}$$

Similarly, the temperatures of the other nodes of the insulator (s_2, s_3, and s_4) can be written as:

$$T_2 = T_c - \frac{T_c - T_{in}}{haz} b_1 \tag{7}$$

$$T_3 = T_c - \frac{T_c - T_{in}}{haz} b_2 \tag{8}$$

$$T_4 = T_c - \frac{T_c - T_{in}}{haz} b_3 \tag{9}$$

where,

$$b_1 = \frac{1}{k_z} \ln \frac{r_l}{r_c} + \frac{1}{k_{ins}} \ln \frac{r_{s2}}{r_l} \quad ,$$

$$b_2 = \frac{1}{k_z} \ln \frac{r_l}{r_c} + \frac{1}{k_{ins}} \ln \frac{r_{s3}}{r_l} \quad \text{, and}$$

$$b_3 = \frac{1}{k_z} \ln \frac{r_l}{r_c} + \frac{1}{k_{ins}} \ln \frac{r_{s4}}{r_l}$$

The heat escaped from the charge towards the cooling coil through the crucible wall and the insulator can be expressed as:

$$Q_l = \frac{2\pi l_w (T_c - T_{in})}{haz} \tag{10}$$

b- Cooling Coil:

The temperature of the water at the outlet of the cooling coil can be expressed in terms of mass flow rate of the cooling water (M_w), the temperature of the water at the inlet of cooling coil (T_{in}), the heat transferred from the charge towards the cooling coil through the crucible wall and the insulator (Q_l), and the power lost in the induction coil as:

$$T_{out} = T_{in} + \frac{qhc + Q_l}{C_{pw}.M_w} \tag{11}$$

c- Induction Coil:

The equivalent heat supplied at the terminals of the coil can be expressed in terms of the electrical power at the terminals of the coil as:

$$P_{acl} = p_t t \tag{12}$$

where, (p_t) is the electrical power supplied to the coil.

IV- MEASUREMENTS AND STATE VECTORS:

Arranging all the above defined measurements into a vector called "*Z*", a system model in terms of the state variable vector "*X*", can be represented in a general compact form as:

$$Z = f(X) \tag{13}$$

Where, f(*X*) indicates the 10 measurement equations, i.e., Nm = 10.

$$Z = [T_1, T_2, T_3, T_4, Q_l, p_t, P_{acl}, M_w, T_{in}, T_{out}] \tag{14}$$

The three elements of the state vector *X*, i.e., Ns = 3, are given by:

$$X = [p_t, M_w, T_{in}] \tag{15}$$

Thus, the measurement redundancy is 3.33

The temperature distribution inside the charge is immeasurable. It is necessary to establish five equations in order to predict the temperatures of the five nodes as mentioned in section II. The equations can be found by considering steady-state radial heat transfer conditions from the surface of the charge, i.e., the outer radius, by using the equation of cylindrical heat transfer with heat generation at the surface, so the temperatures can be expressed as:

$$T_{ci} = T_c - \frac{P_6}{4 * k_c}(r_c^{\,2} - r_{ci}^2) \tag{16}$$

Where, *i* = 1, 2, 3, 4, and 5, and P_6 is the power generation at the surface of the charge per unit volume.

V- THE ESTIMATOR:

The first step of the estimator is the data prefiltering in which data validation will be evaluated and substantiated. The data prefiltering usually consists of limit checking, simple logic comparisons between redundant measurements of essentially the same variables, and averaging a number of relative measurements as a representative one. This process is important before the estimation process is implemented in order to reject bad data (BD) entering the estimation process.

After the data prefiltering process, the measurements enter the estimation process. The WLS approach is adopted here because it is effective and can display a good filtering performance without prior knowledge of the probability density function of the estimates, which is required by other methods [2]. The WLS algorithm is designed on the assumption that the measurement noise has a Gaussian distribution. A statistical test for BD detection is carried out immediately after the estimation process. If BD is detected, identification is needed to detect the location of the BD in the measurement vector.

a- The estimation Algorithm:

Based on the measurement equations developed in section III, the measurements can be modeled as the combination of the actual measurements and the measurement noises, so the measurement process can be expressed as:

$$Z = f(X) + \theta \tag{17}$$

The elements of θ are Gaussian distribution random variables with zero mean and one standard deviation (σ). The WLS takes the following iterative form [6]:

$$\Delta X^* = [\,[H]^T[R]^{-1}[H]\,]^{-1}\,[H]^T\,[R]^{-1}\,[Z - f(X)] \tag{18}$$

Where [H] is the Jacobian matrix and is given by:

$$[H] = \frac{\partial f(X)}{\partial X} \tag{19}$$

The weighted matrix [R] is $(\sigma_1^2, \sigma_2^2, ..., \sigma_m^2)$ diagonal matrix, and the elements give an indication of the accuracy of the corresponding measurements. The iterations continue until a tolerance $\left| x_i^{k+1} - x_i^k \right| < \varepsilon$ is satisfied where the superscript k denotes the iteration cycle.

b- Bad Data Detection:

Bad data detection is carried out by using a statistical criterion known as J-index test [7]. It is based on the measurement residual and standard deviation of each individual measurement. The measurement residual vector (r) is the deviation between the measurements and the estimates and can be written as:

$$r = Z - f(X) \tag{20}$$

The value of the J-index is the statistical variable that is defined as the sum of the weighted squares of all the measurement residuals [7]. This definition is expressed as:

$$J(x) = \sum_{i=1}^{Nm} \frac{r_i^2(i)}{\sigma_i^2} \tag{21}$$

J(x) is a chi-square distribution with a degree of freedom of the measurements equal to the difference between number of measurements and number of states. The detection threshold value t_j can be determined from the chi-square distribution tables after the significance level (α) is specified. If *J(x)* is smaller than t_j, then the resultant estimate is treated as free of BD. However, when the value of *J(x)* is higher than the threshold, it is assumed that there is some BD in the measurements. The process of BD identification is then started.

c- Bad Data Identification:

In order to appoint the location of the bad data, consider the measurement of temperature of a particular part. Call this measured value z_i, which has a corresponding calculated temperature f_i which is a function of the estimated state. The difference between the estimate, f_i, and the measurement, z_i, is called the measurement residual and is designated r_i. The probability density function for r_i is normal and having zero mean and a standard deviation (σ_{ri}). If the measurement residual is divided by (σ_{ri}), a normalized measurement residual is obtained which is designated as r_i^{norm}.

The computational procedure is to calculate the normalized measurement residuals r_i^{norm} for each measurement. Measurements having the larger absolute normalized residual are labeled as prime suspects. These prime suspects are removed from the estimator and can be replaced by their corresponding pseudo measurements [7]. This procedure can be expressed mathematically as:

$$r_i^{norm} = \frac{z_i - f_i(x^*)}{\sigma_{yi}} \tag{22}$$

VI- Testing Indices:

The estimation results can be compared by a statistical test. In order to assess the performance of the estimator, two statistical indices S_e and S_m are used as defined below [8]:

$$S_e = \left[\frac{1}{Nm} \sum_{i=1}^{Nm} \left(\frac{z_{ei} - z_{ti}}{\sigma_i} \right)^2 \right]^{1/2} \tag{23}$$

$$S_m = \left[\frac{1}{Nm} \sum_{i=1}^{Nm} \left(\frac{z_{mi} - z_{ti}}{\sigma_i} \right)^2 \right]^{1/2} \tag{24}$$

When $S_e < S_m$ it shows that the estimator is effective in the filtering process.

VII- Results And Discussion:

A number of computer runs are made in order to test the estimator robustness, each test consist of a comparison between the true and the estimated values for all the variables in the measurement vector Z. The values of the measurement vector Z are taken from Ref. [13] and the algorithm of solution is illustrated by the flow chart shown in Fig. 3. The results showed that for an aluminum charge when the measurements suffer only from the Gaussian noise, the estimator has predicts the charge node temperatures with 0.699% error, table (1). Another test is made when all the measurements have an error of one standard deviation of 5% of the true value, and the estimator still works efficiently with a maximum node error of 1.88%, the results are shown in table (2). For iron charge when the measurements suffer the same two conditions above, the estimator has predicts the charge node temperatures with an error of 0.928%, and 2.099% as illustrated in tables (3) and (4) respectively.

The real evaluation of the robustness of the estimator is when there is a bad data in the measurements. So the estimator was tested by feeding a single bad data of 25% of the true value for an the iron charge, even with this bad data the estimator works efficiently and estimated the charge node temperatures with a 2.13% maximum error as shown in table (5).

Another test for the estimator efficiency with bad data was made by feeding of two and three bad data which are T_{s3} & T_{s4}, and T_{s2}, T_{s3} & T_{s4} as indicated in tables (6) and (7) respectively. The results show that the estimator works with the aluminum as a paramagnetic material more efficient than with the iron. This is because the effect of the Curie point and its influence on the permeability which has a significant effect on the power generation and heating rate. Of course it will work efficiently with the diamagnetic materials because the absence of the Curie point effect just likes the paramagnetic materials.

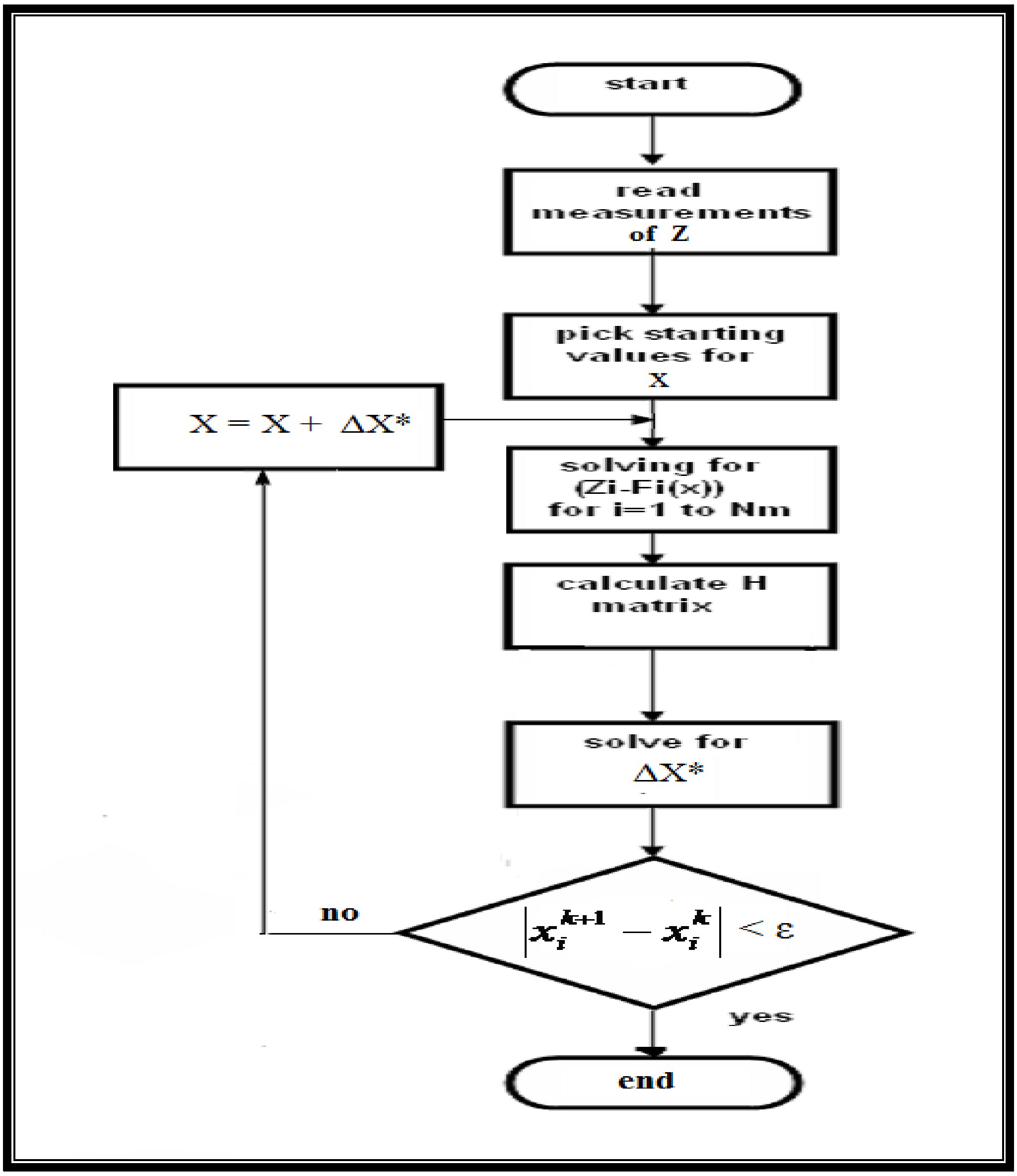

Fig. (3): State estimation solution algorithm

References:

1. Baker R. M., "Classical heat flow problems applied to induction billet heating", AIEE Trans., Vol. 77, pp. 106-112, 1958.
2. Lenden B., Hamza M. H., and Sheirah M. A., " Different methods for estimating thermal diffusivity of a heat process", Automatica, Vol. 12, pp. 445-456, 1976.
3. Potapov I. N., Leibenzon A. S., Shamanaev V. I., and Sobol A. A., "Mathematical model of induction heating of solid round billet", Steel in the USSR, Vol. 16, No. 5, pp. 244-245, 1986.

4. Al-Ubaidy M. A. J., "Charge temperature estimation of an induction furnace", M. Sc. Thesis, Al-Nahrain University, 1994.
5. Ben-Yaacov G. Z., and Bohn J. G., " Methodology for real time calculation of temperature rise and dynamic rating for distribution system duct banks", IEEE Transactions on Power Apparatus and Systems, Vol. PAS-101, No.12, pp. 4604-4610, 1985.
6. Michael A. Chapman, " Adaptation And Installation of a robust state estimation package in the EEF utility", M. Sc. Thesis, Virginia Polytechnic Institute, 1999.
7. Mili L., Van Cutsem T.,and Ribbens-Pavella M., "Bad data identification methods in power system state estimation – A Comparative study", IEEE Transactions on Power Apparatus and Systems, Vol. PAS-104, No.11, pp. 3037-3049, 1985.
8. Lo K. L., Song Z. M., Marchand E., and Pinkerton A., " Development of a static state estimator for a power station boiler, Parts I and II", Electric Power Systems research, Vol. 18, pp. 175-203, 1990.
9. Simpson P. G., " Induction heating coil and system design", McGraw-Hill, 1960.
10. Holman J. P., " Heat transfer", McGraw-Hill, 4th edition, 1976.
11. Charles H. B., and Corrinne P. B., " Understandable statistics concepts and methods", Houghton Mifflin Company, 2003.
12. John B. Moore, " Statistical filtering", Australian Research Committee, 1977.
13. Hazim Wally Chillab, A Study of Static and Dynamic State Observer Applied to an Induction Furnace, M. Sc. Thesis, University of Babylon, College of Engineering, 2008

TABLE (1): ALUMINUM CHARGE WITH GAUSSIAN NOISE, S_e = 0.58638, S_m=.78242 , S_e/S_m = 0.74944 , J(x) = 0.8463, **for all results**; $error\% = \frac{|Z_e - Z_t|}{Z_t} * 100$

Variable	True Value Z_t	Measured Value Z_m	Estimated Value Z_e	Z_m-Z_t	Z_e-Z_t	Error %
T_{s1} (K)	$2.99*10^2$	$3.080*10^2$	$3.034*10^2$	9.00	4.4	
T_{s2} (K)	$4.638*10^2$	$4.661*10^2$	$4.660*10^2$	2.27	2.25	
T_{s3} (K)	$6.355*10^2$	$6.429*10^2$	$6.408*10^2$	7.413	5.32	
T_{s4} (K)	$8.144*10^2$	$8.395*10^2$	$8.268*10^2$	25.08	12.41	
Q_l (W)	$1.854*10^3$	$1.800*10^3$	$1.819*10^3$	-53.77	-34.72	
P_t (W)	$1.41*10^5$	$1.352*10^5$	$1.376*10^5$	$-5.67*10^3$	$-3.40*10^3$	
P_{acl} (J)	$2.961*10^8$	$2.92*10^8$	$2.894*10^8$	$-5.92*10^6$	$-6.23*10^6$	
M_w (kg/s)	2.3	2.3879	2.354	0.0879	0.054	
T_{in} (K)	$2.98*10^2$	$3.117*10^2$	$3.098*10^2$	13.74	11.8	
T_{out} (K)	$2.982*10^2$	$3.124*10^2$	$3.104*10^2$	14.23	12.2	
T_{c1} (K)	$9.531*10^2$	__	$9.466*10^2$	__	-6.516	0.68
T_{c2} (K)	$9.607*10^2$	__	$9.539*10^2$	__	-6.725	0.69
T_{c3} (K)	$9.735*10^2$	__	$9.673*10^2$	__	-6.118	0.62
T_{c4} (K)	$9.913*10^2$	__	$9.853*10^2$	__	-5.971	0.60
T_{c5} (K)	$1.014*10^3$	__	$1.008*10^3$	__	-5.366	0.53

TABLE (2): ALUMINUM CHARGE WITH ERROR OF ONE STANDARD DEVIATION FOR ALL THE MEASUREMENTS, S_e =0.6856 , S_m=1, S_e/S_m = 0.6856, J(x) = 0.92025.

Variable	True Value Z_t	Measured Value Z_m	Estimated Value Z_e	Z_m-Z_t	Z_e-Z_t	Error %
T_{s1} (K)	$2.99*10^2$	$3.139*10^2$	$3.112*10^2$	14.95	12.27	
T_{s2} (K)	$4.638*10^2$	$4.870*10^2$	$4.803*10^2$	23.19	16.49	
T_{s3} (K)	$6.355*10^2$	$6.672*10^2$	$6.597*10^2$	31.77	24.23	
T_{s4} (K)	$8.144*10^2$	$8.551*10^2$	$8.476*10^2$	40.72	33.13	
Q_l (W)	$1.854*10^3$	$1.761*10^3$	$1.792*10^3$	-92.71	-61.64	
P_t (W)	$1.41*10^5$	$1.339*10^5$	$1.364*10^5$	$-7.05*10^3$	$4.60*10^3$	
P_{acl} (J)	$2.961*10^8$	$2.812*10^8$	$2.876*10^8$	$-1.48*10^7$	$-8.4*10^6$	
M_w (kg/s)	2.3	2.415	2.361	0.115	0.061	
T_{in} (K)	$2.98*10^2$	$3.129*10^2$	$3.103*10^2$	14.9	12.3	
T_{out} (K)	$2.982*10^2$	$3.131*10^2$	$3.108*10^2$	14.91	12.6	
T_{c1} (K)	$9.531*10^2$	—	$9.374*10^2$	—	-15.76	1.65
T_{c2} (K)	$9.607*10^2$	—	$9.426*10^2$	—	-18.13	1.88
T_{c3} (K)	$9.735*10^2$	—	$9.582*10^2$	—	-15.25	1.56
T_{c4} (K)	$9.913*10^2$	—	$9.796*10^2$	—	-11.75	1.18
T_{c5} (K)	$1.014*10^3$	—	$1.004*10^3$	—	-9.698	0.95

TABLE (3): IRON CHARGE WITH GAUSSIAN NOISE, S_e = 0.63248, S_m = 0.78351, S_e/S_m = 0.80723, J(x) =1.09267

Variable	True Value Z_t	Measured Value Z_m	Estimated Value Z_e	Z_m-Z_t	Z_e-Z_t	Error %
T_{s1} (K)	$3.89*10^2$	$4.006*10^2$	$3.992*10^2$	11.67	10.32	
T_{s2} (K)	$6.825*10^2$	$7.087*10^2$	$6.999*10^2$	26.22	17.43	
T_{s3} (K)	$1.080*10^3$	$1.116*10^3$	$1.102*10^3$	36.73	22.6	
T_{s4} (K)	$1.493*10^3$	$1.540*10^3$	$1.526*10^3$	47.18	32.93	
Q_l (W)	$4.729*10^3$	$4.604*10^3$	$4.637*10^3$	-124.28	-91.47	
P_t (W)	$1.41*10^5$	$1.367*10^5$	$1.388*10^5$	$-4.23*10^3$	$-2.11*10^3$	
P_{acl} (J)	$8.03*10^8$	$7.84*10^8$	$8.01*10^8$	$-1.9*10^7$	$-2.1*10^6$	
M_w (kg/s)	2.3	2.402	2.36	0.102	.06	
T_{in} (K)	$2.98*10^2$	$3.127*10^2$	$3.120*10^2$	14.7	14.01	
T_{out} (K)	$2.985*10^2$	$3.133*10^2$	$3.128*10^2$	14.81	14.3	
T_{c1} (K)	$1.842*10^3$	—	$1.825*10^3$	—	-17.12	0.92
T_{c2} (K)	$1.864*10^3$	—	$1.846*10^3$	—	-17.28	0.92
T_{c3} (K)	$1.899*10^3$	—	$1.882*10^3$	—	-16.81	0.88
T_{c4} (K)	$1.949*10^3$	—	$1.933*10^3$	—	-15.95	0.81
T_{c5} (K)	$2.013*10^3$	—	$1.997*10^3$	—	-15.61	0.77

TABLE (4): IRONCHARGE WITH ERROR OF ONE STANDARD DEVIATION FOR ALL THE MEASUREMENTS, S_e=0.76541, S_m=1, S_e/S_m=0.76541, J(x) =1.1836

Variable	True Value Z_t	Measured Value Z_m	Estimated Value Z_e	Z_m-Z_t	Z_e-Z_t	Error %
T_{s1} (K)	$3.89*10^2$	$4.084*10^2$	$4.066*10^2$	19.45	17.61	
T_{s2} (K)	$6.825*10^2$	$7.166*10^2$	$7.092*10^2$	34.12	26.7	
T_{s3} (K)	$1.080*10^3$	$1.134*10^3$	$1.117*10^3$	54.51	37.51	
T_{s4} (K)	$1.493*10^3$	$1.567*10^3$	$1.546*10^3$	74.66	53.42	
Q_l (W)	$4.729*10^3$	$4.492*10^3$	$4.577*10^3$	-236.45	-151.61	
P_t (W)	$1.41*10^5$	$1.339*10^5$	$1.357*10^5$	$-7.05*10^3$	$-5.27*10^3$	
P_{acl} (J)	$8.03*10^8$	$7.628*10^8$	$7.94*10^8$	$-4.09*10^7$	$-9.4*10^6$	
M_w (kg/s)	2.3	2.415	2.37	0.115	0.07	
T_{in} (K)	$2.98*10^2$	$3.129*10^2$	$3.122*10^2$	14.9	14.2	
T_{out} (K)	$2.985*10^2$	$3.134*10^2$	$3.131*10^2$	14.92	14.56	
T_{c1} (K)	$1.842*10^3$	—	$1.808*10^3$	—	-34.04	1.84
T_{c2} (K)	$1.864*10^3$	—	$1.825*10^3$	—	-39.14	2.09
T_{c3} (K)	$1.899*10^3$	—	$1.866*10^3$	—	-33.43	1.76
T_{c4} (K)	$1.949*10^3$	—	$1.920*10^3$	—	-29.23	1.49
T_{c5} (K)	$2.013*10^3$	—	$1.984*10^3$	—	-28.18	1.39

TABLE (5): IRON CHARGE WITH SINGLE BAD DATA, S_e = 0.67531, S_m = 0.9486, S_e/S_m = 0.7119, J(x) = 20.6491

Variable	True Value Z_t	Measured Value Z_m	Estimated Value Z_e	Z_m-Z_t	Z_e-Z_t	Error %
T_{s1} (K)	$3.89*10^2$	$4.006*10^2$	$4.048*10^2$	11.67	15.82	
T_{s2} (K)	$6.825*10^2$	$7.087*10^2$	$7.014*10^2$	26.22	18.9	
T_{s3} (K)	$1.080*10^3$	810.15	$1.056*10^3$	-270.05	-23.89	
T_{s4} (K)	$1.493*10^3$	$1.540*10^3$	$1.537*10^3$	47.18	43.78	
Q_l (W)	$4.729*10^3$	$4.604*10^3$	$4.648*10^3$	-124.28	-80.18	
P_t (W)	$1.41*10^5$	$1.367*10^5$	$1.372*10^5$	$-4.23*10^3$	$-3.8*10^3$	
P_{acl} (J)	$8.03*10^8$	$7.84*10^8$	$7.96*10^8$	$-1.9*10^7$	$-7.6*10^6$	
M_w (kg/s)	2.3	2.402	2.366	0.102	0.066	
T_{in} (K)	$2.98*10^2$	$3.127*10^2$	$3.12*10^2$	14.7	14.07	
T_{out} (K)	$2.985*10^2$	$3.133*10^2$	$3.129*10^2$	14.81	14.44	
T_{c1} (K)	$1.842*10^3$	—	$1.807*10^3$	—	-35.25	1.91
T_{c2} (K)	$1.864*10^3$	—	$1.824*10^3$	—	-39.68	2.13
T_{c3} (K)	$1.899*10^3$	—	$1.865*10^3$	—	-34.16	1.79
T_{c4} (K)	$1.949*10^3$	—	$1.918*10^3$	—	-30.44	1.56
T_{c5} (K)	$2.013*10^3$	—	$1.984*10^3$	—	-28.97	1.44

TABLE (6): IRON CHARGE WITH TWO BAD DATA, S_e = 1.4857 , S_m = 2.2471 , S_e/S_m = 0.6619 , J(x) = 31.4054

Variable	True Value Z_t	Measured Value Z_m	Estimated Value Z_e	Z_m-Z_t	Z_e-Z_t	Error %
T_{s1} (K)	$3.89*10^2$	$4.006*10^2$	$3.615*10^2$	11.67	-27.64	
T_{s2} (K)	$6.825*10^2$	$7.087*10^2$	$6.462*10^2$	26.22	-36.29	
T_{s3} (K)	$1.080*10^3$	0.00	$1.028*10^3$	-83	-51.47	
T_{s4} (K)	$1.493*10^3$	0.00	[illegible]	-495.4	-63.98	
Q_l (W)	$4.729*10^3$	$4.604*10^3$	[illegible]	-124.28	-139.9	
P_t (W)	$1.41*10^5$	$1.367*10^5$	$1.356*10^5$	$-4.23*10^3$	-5350	
P_{acl} (J)	$8.03*10^8$	$7.84*10^8$	$7.62*10^8$	$-1.9*10^7$	$-4.17*10^7$	
M_w (kg/s)	2.3	2.402	2.407	0.102	0.107	
T_{in} (K)	$2.98*10^2$	$3.127*10^2$	$3.129*10^2$	14.72	14.9	
T_{out} (K)	$2.985*10^2$	$3.133*10^2$	$3.134*10^2$	14.81	14.93	
T_{c1} (K)	$1.842*10^3$	—	$1.782*10^3$	—	-60.81	3.3
T_{c2} (K)	$1.864*10^3$	—	$1.797*10^3$	—	-67.11	3.59
T_{c3} (K)	$1.899*10^3$	—	$1.838*10^3$	—	-60.98	3.21
T_{c4} (K)	$1.949*10^3$	—	$1.887*10^3$	—	-61.59	3.16
T_{c5} (K)	$2.013*10^3$	—	$1.953*10^3$	—	-59.99	2.98

TABLE (7): IRON CHARGE WITH THREE BAD DATA, S_e =1.76352, S_m = 2.6683, S_e/S_m = 0.66091, J(x) = 35.5375

Variable	True Value Z_t	Measured Value Z_m	Estimated Value Z_e	Z_m-Z_t	Z_e-Z_t	Error %
T_{s1} (K)	$3.89*10^2$	$4.006*10^2$	$3.552*10^2$	11.67	-33.47	
T_{s2} (K)	$6.825*10^2$	0.00	$6.362*10^2$	-281.8	-46.25	
T_{s3} (K)	$1.080*10^3$	0.00	$1.010*10^3$	-679.5	-69.45	
T_{s4} (K)	$1.493*10^3$	0.00	$1.411*10^3$	-1092.63	-82.07	
Q_l (W)	$4.729*10^3$	$4.604*10^3$	$4.576*10^3$	-124.28	-152.5	
P_t (W)	$1.41*10^5$	$1.367*10^5$	$1.354*10^5$	$-4.23*10^3$	$-5.60*10^3$	
P_{acl} (J)	$8.03*10^8$	$7.84*10^8$	$7.625*10^8$	$-1.9*10^7$	$-4.11*10^7$	
M_w (kg/s)	2.3	2.402	2.409	0.102	0.109	
T_{in} (K)	$2.98*10^2$	$3.127*10^2$	$3.130*10^2$	14.7	15.07	
T_{out} (K)	$2.985*10^2$	$3.133*10^2$	$3.136*10^2$	14.81	15.08	
T_{c1} (K)	$1.842*10^3$	—	$1.760*10^3$	—	-82.17	4.46
T_{c2} (K)	$1.864*10^3$	—	$1.774*10^3$	—	-89.66	4.81
T_{c3} (K)	$1.899*10^3$	—	$1.816*10^3$	—	-82.85	4.36
T_{c4} (K)	$1.949*10^3$	—	$1.866*10^3$	—	-83.16	4.26
T_{c5} (K)	$2.013*10^3$	—	$1.931*10^3$	—	-81.48	4.04

NOMENCLATURE:

C : Effective thermal capacitance.

C_p: Specific heat of the charge. kJ/kg.^oK

C_{pw}: Specific heat of water. kJ/kg.^oK

[H]: Jacobian matrix.

k_c, k_{cu}, k_{ins}, k_z: Thermal conductivity of charge material, copper, insulator material and zircon material, respectively. W/m.^oK

M_c : Mass of the charge. kg

M_w: Mass flow rate of the water. kg/s

Nm : Number of the measurements

Ns : Number of the state variables

P_{acl} : Equivalent heat supplied at the terminals of the coil. kJ

p_t : Electrical power supplied to the coil. kW

Q_l : Heat escaped from the charge towards the cooling coil. kW

qhc : Coil power loss. kW

q_i : Power generated at a node. kW

R: Effective thermal resistance

[R] : Weighted matrix

r_c: Radius of the charge. m

r_{ins}: Radius of the end of insulator. m

r_j : The measurement residual

r_l : Radius of the end of the refractory. m

r_{s1}, r_{s2}, r_{s3}, r_{s4} : Radii of nodes s_1-s_4

r_w : Radius from center to the cooling coil. m

S_e: Statistical index of the estimates

S_m: Statistical index of the measurements

T: Temperature. ^oK

T_a: Temperature at adjacent node. ^oK

T_c : Charge surface temperature. ^oK

T_{in}: Water temperature at cooling coil inlet. ^oK

$T_{initail}$: Initial charge temperature. ^oK

T_{out} : Water temperature at cooling coil outlet. ^oK

T: Time. s

t_j : Detection threshold

X : State vector

y_i^{norm} : Normalized measurement residual

Z: Measurement vector

z_e : Estimated value

z_m: Measured value

z_t: True value

θ: Measurements noise

ρ: Charge density. kg/m^3